



Step enhanced dehydrogenation of ethanol on Rh

Andrea Resta^a, Johan Gustafson^a, Rasmus Westerström^a, Anders Mikkelsen^a, Edvin Lundgren^a, Jesper N. Andersen^{a,*}, Ming-Mei Yang^b, Xiu-Fang Ma^b, Xin-He Bao^b, Wei-Xue Li^b

^a Department of Synchrotron Radiation Research, Institute of Physics, Lund University, Box 118, S-22100 Lund, Sweden

^b State Key Laboratory of Catalysis, Dalian Institute of Chemical Physics, Chinese Academy of Sciences, 457 Zhongshan Road, Dalian 116023, China

ARTICLE INFO

Article history:

Received 18 June 2008

Accepted for publication 5 August 2008

Available online 14 August 2008

Keywords:

Density functional calculations

Photoelectron spectroscopy, soft X-ray

photoelectron spectroscopy, synchrotron

radiation photoelectron spectroscopy

Chemisorption

Catalysis

Surface chemical reaction

Rh, ethanol, methylidyne, ethylidyne, C, CO,

H

ABSTRACT

We have investigated the adsorption and decomposition of ethanol on the Rh(111) and Rh(553) surfaces at room temperature with special emphasis on the dehydrogenation. We use high resolution core level photoemission and density functional theory (DFT) based simulations. A detailed analysis of the C1s core level spectra, including analysis of the vibrational fine-structure and comparison to calculated C1s binding energy shifts, shows that the ethanol decomposes into CO, ethylidyne (C₂H₃), methylidyne (CH), atomic C, and hydrogen. At low ethanol exposures, CH is the dominating hydrocarbon fragment on Rh(111), whereas on Rh(553) atomic C dominates over CH, indicating an enhanced dehydrogenation due to the steps present on the latter surface. At higher ethanol exposures we find a similar behavior of atomic C dominating over hydrocarbons on Rh(553), while on Rh(111) atomic carbon remains a minority species. Our DFT based simulations show that the enhanced dehydrogenation results from a significant lowering of the CH dissociation barrier from Rh(111) to Rh(553), as well as from the dissociation changing from endothermic on Rh(111) to exothermic on Rh(553).

© 2008 Elsevier B.V. All rights reserved.

1. Introduction

Hydrogen is being considered as a possible major energy source for the future, to be used in fuel cells where the hydrogen is oxidized into H₂O and electricity is produced. Storage of pure hydrogen, however, presents severe safety-related problems and it has therefore been suggested to store and transport the hydrogen in the form of a more stable hydrogen-containing compound from which the hydrogen is extracted in close proximity to its use in e.g. fuel cells. One such H-containing compound under consideration is ethanol, for which it has recently [1–4] been demonstrated that Rh-ceria based catalytic extraction of hydrogen by partial oxidation is possible at relatively low temperatures.

However, little is known about the reasons for the efficiency of the Rh-ceria based catalysts used for H₂ production. This applies not only to the partial-oxidation reaction but even to the fundamental steps of ethanol adsorption [5] and fragmentation on Rh surfaces. As edges and corners constitute a significant fraction of the surface area in the small Rh particles typically used in real catalysts, it is important to investigate what influence the presence of under-coordinated Rh atoms has on ethanol adsorption and fragmentation. We have therefore studied the room temperature

adsorption and decomposition of ethanol on both the flat Rh(111) and the vicinal Rh(553) surfaces where the steps on the latter are used to mimic, at least partly, the under-coordinated atoms present at the edges and corners of small Rh particles. Our results show significantly different fragmentation of ethanol on these two surfaces, demonstrating a large influence of the under-coordinated step atoms at the 111-type microfacets of the Rh(553) surface. On both surfaces, we find that predominantly the C–C as opposed to the C–O bond of the ethanol molecule is broken due to the interaction with Rh. However, on the flat Rh(111) surface, hydrocarbons constitute a large fraction of the final decomposition products indicating non-complete dehydrogenation whereas on Rh(553) an atomic carbon species is found to dominate over hydrocarbon fragments indicating a more complete dehydrogenation at the steps. The enhanced dehydrogenation at the steps is shown to be the result of both a significantly lower energy barrier for CH dissociation as well as the dehydrogenation becoming exothermic at the steps.

In addition to providing information on ethanol adsorption and decomposition on Rh(111) and Rh(553), the present study also demonstrates the potential of high resolution core level spectroscopy (HRCLS) for identifying hydrocarbon fragments on surfaces. This potential, which is not restricted to the current Rh surfaces, rests on a detailed analysis of the vibrational fine structure present in the HRCLS C1s spectra of adsorbed hydrocarbons and on

* Corresponding author. Tel.: +46 46 222 4153; fax: +46 46 222 4221.

E-mail address: jesper.andersen@sljus.lu.se (J.N. Andersen).

comparison to theoretical simulations of adsorption structures and C1s binding energy shifts [6–9].

2. Experimental and calculational details

The measurements were performed at beam line I311 at the synchrotron radiation facility MAX II in Lund, Sweden. We refer the reader to Ref. [10] for a detailed description of this beam line. Experimental procedures were as described in Ref. [11]. In short, the surfaces were cleaned by a combination of Ar⁺ sputtering and annealing in O₂ and in vacuum. The surface cleanliness was checked by HRCLS and the long range order by low energy electron diffraction (LEED). The HRCL spectra were recorded at normal emission and at liquid nitrogen temperatures in order to reduce thermal broadenings. Special attention was paid to the possibility of beam induced dissociation due to the high incident flux. No such effects were found for the present experimental conditions.

Ethanol exposures are given in Langmuir (L) (1 L = 10⁻⁶ torr s) based on the gauge reading with no correction applied for the sensitivity towards ethanol [12]. Ethanol pressures in the low 10⁻⁸ torr range were typically used except for the lowest exposures. The ethanol was 99.5% pure with dry residuals less than 0.002% and was further purified by freeze-pump-thaw cycles.

The HRCL spectra were decomposed using Doniach–Sunjic line shapes [13] convoluted with Gaussian functions that represent unresolved vibrations and the experimental broadening. A linear background was included in the fits. For the case of hydrocarbons, it has long been known [14] that intrinsic excitation of C–H stretch vibrations in the photoemission process gives rise to higher binding energy satellites in the C1s spectra also for the case of chemisorbed molecules, see e.g. Refs. [6–9]. The energy separation of the C–H vibrational satellites is in all cases close to 400 meV and the intensity distribution closely follows a Poisson distribution as expected from a linear coupling model [15]. For the decomposition of hydrocarbon spectra we have therefore used vibrational components with an energy splitting of close to 400 meV and the additional constraint that the intensities of these components follow a Poisson distribution.

For the slab-based calculations of surface structures we used density functional theory (DFT) as implemented in the DACAPO package [16]. Ion-cores were described by ultrasoft pseudopotentials [17]. In order to describe core ionized C atoms, we used a pseudopotential constructed for a C atom where a 1s electron had been promoted to a 2p valence level [18–21]. The one-electron wave functions were expanded in a plane wave basis with an energy cutoff of 25 Ry. For the exchange and correlation functional we used the generalized gradient approximation (GGA) as implemented in the PW91 form [22]. For Rh(111) we used a three-layer slab and for Rh(553) a slab containing three (111) Rh layers. The first two substrate layers as well as the adsorbates were allowed to relax geometrically. The slabs were separated by vacuum layers of thickness equivalent to five (111) Rh layers. Energy barriers were found by constrained relaxation with care being taken that the pathways become continuous. Sampling of *k*-space was done using a (2 × 4 × 1) mesh for the (5 × 2) and (1 × 2) unit cells used for Rh(111) and Rh(553), respectively. The theoretical lattice constant 3.83 Å was used for Rh. Finally, the C1s core level binding energy shifts were calculated as total energy differences between systems where the appropriate C-atoms had been core-ionized. Convergence tests showed that increasing the slab thickness from three to five layers caused the relative differences of the adsorption energies for atomic C and CH at different sites to change by less than 50 meV. Changes of the corresponding C1s core level shifts were less than 10 meV. The conclusions based on three layer slabs are therefore not affected.

3. Results and discussion

C1s spectra measured after representative room temperature ethanol exposures ranging from 0.1 to 30 L on Rh(111) and Rh(553) are shown in Fig. 1a and b, respectively, together with decompositions into a number of components.

3.1. C1s results, overview

The C1s peaks at binding energies above 285 eV can all be assigned to CO molecules adsorbed in different sites on the two surfaces. For Rh(111) the components at ~286 and ~285.4 eV are assigned to CO molecules in on-top and three-fold-hollow adsorption sites, respectively, based upon their binding energies, as discussed in more detail in [11]. The shoulder at ~286.3 eV on the high binding energy side of the on-top peak is due to the intrinsic excitation of the C–O stretch vibration in the photoemission process [23] and not to CO in a different configuration. For Rh(553), the C1s components at similar binding energies as those found on Rh(111) are interpreted as due to CO molecules in on-top and three-fold-hollow sites on the (111) terraces of the surface. In addition, a C1s component at ~285.7 eV is clearly visible after ethanol exposures up to 1 L. This component can, by comparison to C1s spectra measured after CO exposure of Rh(553) [24], be ascribed to CO molecules adsorbed on-top the Rh atoms at the steps

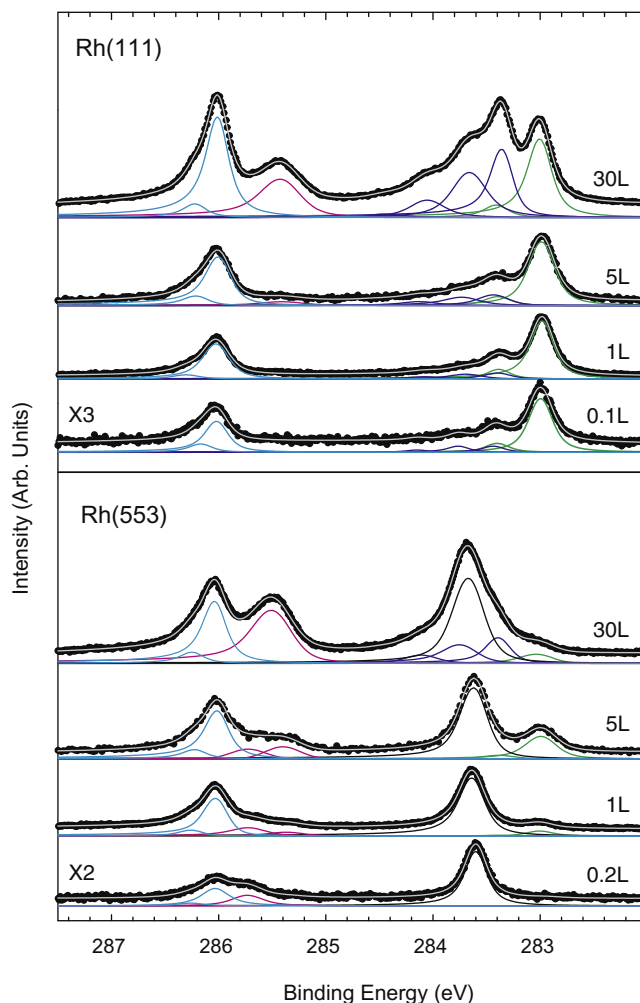


Fig. 1. C1s spectra after ethanol exposures at room temperature between 0.1 and 30 L on Rh(111) and Rh(553). The photon energy is 380 eV. Decompositions of the spectra into a number of components as explained in the text are shown.

of Rh(553). For the sake of simplicity we include an explicit component for this step-adsorbed CO only at the lower ethanol exposures whereas at higher exposures we incorporate it via an additional broadening of the three-fold-hollow component.

As discussed previously [11], the above assignments for Rh(111) are supported by corresponding O1s spectra. We find the O1s spectra for Rh(553) to be very similar to those for Rh(111). In particular we find a similar lack of any emission around 529.5 eV which could be ascribed to atomic oxygen. From this, and the appearance of CO on the surface, we conclude that the C–C bond of the ethanol molecule is broken upon adsorption on Rh surfaces at 300 K whereas the C–O bond is left intact.

The remaining C1s components are all found at binding energies between ~ 283 and ~ 284.5 eV, that is, in the binding energy range expected for hydrocarbons and/or for C-species adsorbed on metallic surfaces see e.g. [6–9,25–27]. Assigning these components to specific molecular fragments is in general difficult due to the large number of possible C–H containing fragments, the close-lying and even overlapping C1s binding energies, and the possibility that some of the components are not due to chemical shifts but instead to the excitation of C–H vibrations in the photoemission process. In the present case we, however, believe that several fragments can be unambiguously identified.

3.2. Rh(111), the hydrocarbon region

We start with the Rh(111) surface and ethanol exposures of up to 5 L, see Fig. 1a. For these exposures, the C1s spectra below 285 eV binding energy contain two main components; one at 283.0 eV and one at 283.4 eV. In addition, a broad shoulder is visible, in particular at 5 L exposure, on the high binding energy side of the 283.4 eV component. In a previous publication [11] it was tentatively suggested that the 283 eV component was due to atomic C on the surface based on its low binding energy. Here we show that instead this component is the adiabatic peak from CH (methylidyne) fragments on the surface and that part of the 283.4 eV peak is due to excitation of the C–H stretch vibration of the CH molecule.

A priori the emission at 283.4 eV could be either a chemically shifted C1s component or, as it is shifted ~ 400 meV from the 283.0 eV component, a vibrational shake-up of the C–H stretch in the hydrocarbon fragment, or a combination of these two possibilities. In order to distinguish between these possibilities we performed experiments where fully deuterated ethanol was used as this should reduce [6,15] the C–H vibrational energy by close to the factor of $\sqrt{2}$ expected for a harmonic oscillator, i.e. the component should shift from 283.4 to 283.3 eV. As seen from Fig. 2, deuteration causes the 283.4 eV peak to split into two components, one at just above 283.4 eV and one at 283.3 eV where the 283.3 eV component can be identified as due to the excitation of a C–D stretch vibration. The component at just above 283.4 eV in the deuterated spectra is due to a chemically shifted component which, as shown below, is ethylidyne (C–CH₃). We thus can conclude that part of the 283.4 eV emission in the non-deuterated spectra of Figs. 1 and 2 is due to a C–H vibrational satellite of the 283.0 eV peak and that the remaining part of the intensity comes from ethylidyne that has a chemically shifted component at that energy.

In identifying that the 283.0 eV component corresponds to methylidyne we make use of the correlation [6–9,28] between the intensity ratio (the so-called *S*-factor) of the first vibrational component and the number of H-atoms bonding to the C-atom. For free molecules [28] and for CH₂ and CH₃ groups in molecules chemisorbed on surfaces [6,7,9], the *S*-factor is found to depend almost linearly on the number of H-atoms bound to the C atom. The proportionality factor is around 0.13 per H-atom for free molecules and for hydrocarbon groups not directly chemisorbed to the metal surface whereas for CH species directly chemisorbed on metal surfaces, a slightly larger *S*-factor of ~ 0.17 is found [9]. In the present case, extraction of the *S*-factor is made difficult by the presence, as described above, of another chemical component overlapping the first C–H vibrational component. However, for the deuterated spectra this difficulty decreases due to the lowering of the C–D vibrational energy which allows separation of the C–D component and quite unambiguous determination of its *S*-factor as being ~ 0.22 , see Fig. 2. As the *S*-factor (for the harmonic

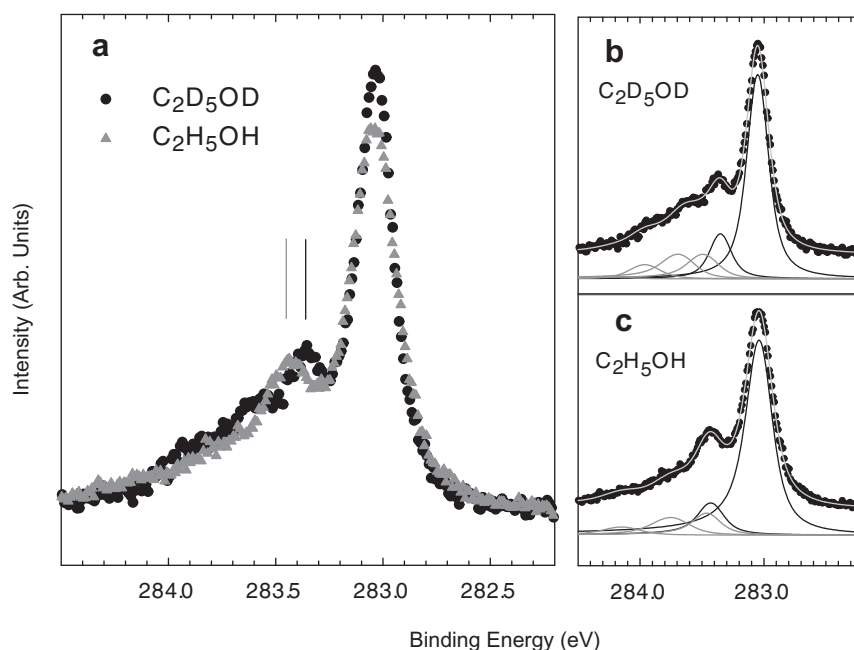


Fig. 2. (a) C1s spectra after exposure of Rh(111) to 0.5 L of ethanol (grey triangles) and deuterated ethanol (black dots), respectively, at room temperature. The shift of the vibrational component upon deuteration is indicated. Decompositions of the C1s spectra after an exposure of 0.5 L deuterated (b) and normal (c) ethanol, respectively. Black lines are adiabatic and vibrational components from methylidyne; grey lines are components due to ethylidyne (see text).

approximation) increases by close to a factor of $\sqrt{2}$ from CH to CD, the 0.22 determined for the deuterated species corresponds to about 0.16 for the non-deuterated case i.e. a value consistent with methylidyne directly bonded to a metal surface. Using this S -factor of 0.16 for the non-deuterated spectra results in fits where the intensity of the additional chemically shifted component at just above 283.4 eV due to ethylidyne is very similar to those found for the deuterated case, see Fig. 2, demonstrating the internal consistency of the assignment and the S -factors. From this analysis we conclude that methylidyne is found on the Rh(111) surface and gives rise to an adiabatic C1s peak at 283.0 eV binding energy and a vibrational satellite at 283.4 eV with intensity around 0.16 times that of the adiabatic peak.

The presence of methylidyne on the surface is further supported by our theoretical calculations which, as described below, show that the dehydrogenation of CH to C is not thermodynamically preferred on Rh(111), and that the activation barrier for this endothermic reaction is about 1 eV. These conclusions are further supported by other recent calculations which show methylidyne to be the most stable CH_x ($1 \leq x \leq 4$) molecule on Rh(111), with a high activation barrier for further dehydrogenation [21,29].

We now turn to the 30 L exposure spectrum in Fig. 1a as an example of the behaviour at higher ethanol doses. In this spectrum we, in addition to what can be ascribed to emission from methylidyne, find strong components at about 283.4, 283.74 and 284.14 eV. We believe these components are due to the formation of ethylidyne on the surface. On Rh(111), the ethylidyne molecule adsorbs with the molecular axis normal to the surface plane in a three-fold-hollow site with the CH_3 group furthest from the surface. The two C-atoms of the molecule have different C1s binding energies. The inner C-atom gives rise to C1s peaks at 283.45 and 283.46 eV [6,7] for the (2×2) -Rh(111)-1CCH₃ and the $c(4 \times 2)$ -Rh(111)-1CO + 1CCH₃ structures, respectively. The adiabatic C1s binding energy of the outer C-atom is found [6,7] at 284.07 and 283.64 eV, respectively. The fact that the outer C-atom is part of a methyl group gives rise to additional C–H vibrational fine-structure components with splittings of ~ 400 meV and an S -factor of ~ 0.4 [6,7]. Finally, the strong variation with photon energy of the outer to inner C-atom intensity ratio provides a reliable fingerprint for the existence of ethylidyne molecules on the surface also when e.g. co-adsorbed with CO [7]. For the present spectra we interpret the ~ 283.4 eV component as due to the inner C-atom, the 283.74 eV component as the adiabatic peak of the outer C-atom, and the 284.14 eV component as the first C–H vibration of the outer C-atom of ethylidyne formed on the surface. Using this assignment we obtain an outer to inner C-atom intensity ratio variation versus photon energy as shown in Fig. 3 (for the 283.4 eV intensity we have subtracted the part accounted for by the vibrational component of methylidyne also found at this energy). Clearly the present intensity variation is very similar to the one found for the $c(4 \times 2)$ -Rh(111)-1CO + 1CCH₃ overlayer, also shown in Fig. 3. In particular we also in the present system find the almost complete suppression of emission from the outer C-atom at 350 eV photon energy, a suppression very characteristic of ethylidyne on Rh(111). Furthermore, use of an S -factor of 0.4 characteristic of a methyl group (and inclusion of the next C–H vibrational feature at 284.53 eV) provides good fits of the spectra. We therefore, based upon the C1s binding energies, the S -factor, and the intensity variation with photon energy assign the 283.4 eV emission as well as the shoulders at 283.74 and 284.14 eV to ethylidyne.

These C1s components from ethylidyne have also been included in the decompositions of the low coverage spectra. In addition to providing a good description of the measured spectra this is justified by the fact that spectra measured at a photon energy of 350 eV (not shown) show reduced emission on the high energy side of the

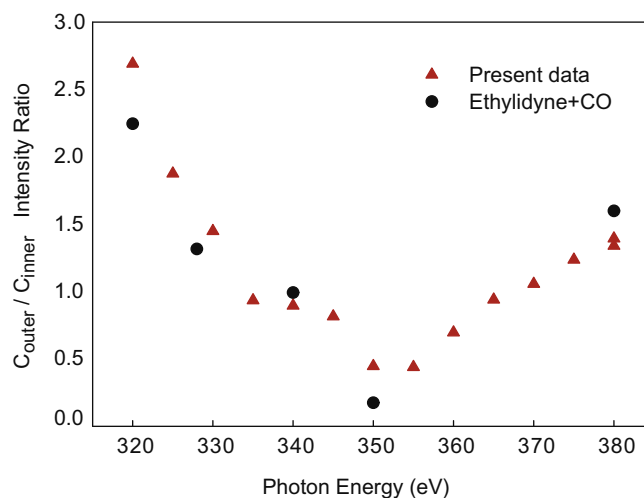


Fig. 3. Comparison of the C1s intensity ratio between the outer (C_{outer}) and the inner (C_{inner}) C-atom of ethylidyne versus photon energy for the present system (red triangles) and ethylidyne co-adsorbed with CO (black dots) from Ref. [7]. (For interpretation of the references to color in this figure legend, the reader is referred to the web version of this article.)

283.4 eV component in agreement with the behaviour of ethylidyne. It should be noticed that the outer to inner C intensity ratio of the ethylidyne components is slightly larger for the lower exposures. In addition to the difficulties in determining exactly the intensity for the inner C-atom due to the overlap with the first vibrational component of the methylidyne, this behaviour could also be caused by the existence of additional low intensity C1s components, e.g. due to molecular fragments formed at steps and other surface defects, not taken into account in the fitting procedure.

Summing up the Rh(111) results, the decomposition of ethanol at temperatures around 300 K results in the formation of CO, methylidyne, and ethylidyne. This, and the fact that no signal attributable to atomic O is observed [11], leads us to conclude that predominantly the C–C bond of the ethanol molecule is broken by the interaction with the Rh-surface. Importantly the spectra can be accounted for without involving any significant emission from atomic carbon species, indicating that dehydrogenation does not proceed beyond the formation of methylidyne.

3.3. Rh(553), the hydrocarbon region

We now turn to Rh(553) and the ~ 283 to ~ 284.5 eV region, see Fig. 1b, in order to investigate the influence of the under-coordinated Rh step atoms on the formation of hydrocarbon and/or atomic C-species.

A dramatic difference is seen when comparing the low ethanol exposure spectra of Fig. 1b for Rh(553) to those for Rh(111) shown in Figs. 1a and 2. Instead of the dominating component at 283 eV and a weak emission at ~ 283.4 eV found for Rh(111), the Rh(553) C1s spectra are dominated by a component at ~ 283.55 eV and a weak component at ~ 283 eV. The dominating component at 283.55 eV is very narrow in energy, has a very small asymmetry, and does not exhibit any satellites that can be attributed to C–H vibrations. This immediately suggests that it is due to some form of atomic C on the surface, although the ~ 0.55 eV higher binding energy than that of CH on Rh(111) is surprisingly high. However, as discussed below, theoretical calculations of the C1s binding energy supports that this component is indeed due to atomic carbon on the surface. The weak component at ~ 283 eV is in analogy with the Rh(111) results interpreted as

due to a small amount of methylidyne on the surface presumably on the (111) terraces of the surface. Thus, in contrast to the situation on Rh(111), the decomposition of ethanol on the stepped Rh(553) surface does not stop at the formation of CH but instead continues to almost complete dehydrogenation of the fragments. This conclusion is supported by our theoretical calculations as discussed below.

The 283.56 eV component remains dominant also at higher ethanol exposures. At the highest exposures, see the 30 L spectrum of Fig. 2, this component broadens and a shoulder develops towards lower binding energy. This can be reproduced if the aforementioned C1s components characteristic for ethylidyne are included. Thus at higher coverages, ethylidyne also forms on Rh(553), most likely on the 111-type terraces of the surface albeit in much smaller quantities than on Rh(111). The ~ 283 eV component ascribed to methylidyne increases between the 1 and 5 L exposures and thereafter decreases. From measurements at intermediate exposures we found that the 283 eV intensity reaches within 90% of its maximum intensity after ~ 2 L exposure, goes through a maximum at ~ 5 L, and drops below the 90% limit at ~ 10 L. As evidenced by the spectra in Fig. 1b, the intensity decrease with ethanol exposure is slower than the initial increase. The initial increase of the 283 eV component may be rationalized as caused by an increasing deactivation of the steps by the 283.55 eV C-species causing the methylidyne dissociation to become less efficient. The decrease of the methylidyne intensity at higher ethanol exposures is accompanied by the appearance of the ethylidyne components. The present data, however, are not sufficient to determine if this is due to conversion of methylidyne to ethylidyne at higher coverages or simply to a new reaction pathway for the ethanol decomposition which also includes a step that converts methylidyne to a different species.

In summary, the decomposition of ethanol on Rh(553) at temperatures around 300 K results in the formation of CO, a dominating atomic C-species, a minor amount of methylidyne, and after high ethanol exposures the formation of ethylidyne. As also found for Rh(111), the lack of an O1s component from atomic O-species indicate predominant C–C bond breaking of the ethanol molecules. Finally, the finding of a significant amount of atomic carbon demonstrates that on Rh(553) dehydrogenation does not stop at the formation of methylidyne.

3.4. Comparison to theoretical results

Comparing the experimental results from Rh(111) and Rh(553), we find that the presence of the under-coordinated step atoms on Rh(553) significantly influences the molecular fragments present after ethanol decomposition at room temperature. With the interpretations of the experimental data given in Sections 3.2 and 3.3, a major reason for the differences is that Rh(553), in particular at low ethanol exposures, very efficiently dissociates CH whereas on Rh(111) the majority of the CH molecules remain intact. Such step-mediated enhanced CH dissociation has also recently been reported for Pt(553) [30]. We have investigated this issue of CH stability further by DFT based simulations. In addition to supporting the above interpretation of a high CH dissociation efficiency at the steps, these calculations also provide an explanation to the high C1s binding energy found for the atomic C-species on Rh(553).

In Table 1, we give the adsorption energies (relative to CH in gas-phase) for fcc and hcp adsorption of CH in a (5×2) -1CH structure on Rh(111) and for CH in various adsorption sites in a (1×2) -1CH structure on Rh(553). Our designations for the various adsorption sites on the Rh(553) surface are shown in Fig. 4. Table 1 also gives the calculated C1s chemical shifts using as reference the C1s binding energy of CH adsorbed in an hcp site in the

Table 1

The adsorption energy (E_{ads}) with respect to a CH radical in gas phase and the C1s core level shifts (CLS) relative to CH in the hcp site on Rh(111) for Rh(111)- (5×2) -1CH and Rh(553)- (1×2) -1CH structures, respectively

Surface	Site	E_{ads} (eV)	CLS (eV)
Rh(111)	Hcp	-6.54	0.00
	Fcc	-6.34	-0.16
Rh(553)	Fcc(up)	-6.58	-0.13
	Hcp(terrace)	-6.55	0.00
	Hcp(up)	-6.53	-0.03
	Hcp(low)	-6.44	0.55
	Fcc(low)	-6.39	0.04
	Fcc(terrace)	-6.28	-0.14
	Step(bridge)	-6.16	-0.12

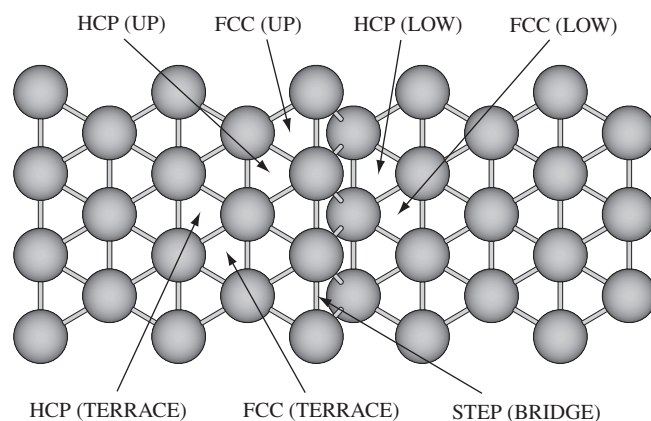


Fig. 4. Top-view of the Rh(553) surface. The designations for the various adsorption sites considered are shown.

Rh(111)- (5×2) -1CH structure. On Rh(111), the hcp site is preferred by the CH molecules, whereas on Rh(553) the two three-fold sites on the upper side of the step and the terrace hcp site all are within 50 meV in adsorption energy. It is therefore not possible to unambiguously choose between these three adsorption sites on the Rh(553). The C1s binding energy is for all of these three sites on Rh(553) within 0.13 eV of the value for CH on Rh(111) which on one hand supports the interpretation that the minority 283.0 eV component on Rh(553) is due to CH but on the other hand also precludes use of the C1s binding energy for distinguishing between the three adsorption sites. Table 1 also shows that a CH molecule adsorbed in the hcp site below the step would actually exhibit a C1s shift of 0.55 eV relative to the (111) hcp site and would therefore be a candidate for the 283.55 eV component. However, in addition to the fact that the calculated adsorption energy for such an adsorption site is 0.14 eV less favourable than the highest adsorption energy, such a suggestion is inconsistent with the experimental observation that the 283.55 eV component is not accompanied by a C–H vibrational satellite.

In Table 2 we give the adsorption energies of a C atom (relative to a C atom in gas-phase) for a (5×2) -1C structure with the C-atom in the (stable) hcp site on Rh(111) and for various adsorption sites in a (1×2) -C structure on Rh(553). For Rh(553), the hcp(low) site is seen to be preferred by at least 0.28 eV per C-atom over other sites and furthermore to give a C1s binding energy shift of 0.46 eV relative to CH in hcp on Rh(111). Thus this adsorption site provides a straightforward explanation for the dominating 283.55 eV peak in the experimental C1s spectra for Rh(553). Calculations for a number of systems with co-adsorbed C and CH show that the hcp(low) site is preferred by C also in such systems and most importantly that the C1s binding energy of the C atom is

Table 2

The adsorption energy (E_{ads}) with respect to a C atom in gas phase and the C1s core level shifts (CLS) relative to CH in the hcp site on Rh(111)–(5 × 2)–1CH for Rh(111)–(5 × 2)–1C and Rh(553)–(1 × 2)–1C structures, respectively

Surface	Site	E_{ads} (eV)	CLS (eV)
Rh(111)	Hcp	–7.18	0.03
Rh(553)	Hcp(low)	–7.54	0.46
	Fcc(up)	–7.00	0.33
	Hcp(up)	–7.26	0.23
	Hcp(terrace)	–7.15	0.05
	Fcc(terrace)	–6.75	0.01
	Fcc(low)	–6.79	0.06
	Bridge(step)	–6.80	0.08

only weakly influenced by co-adsorbed CH. For most co-adsorption geometries, keeping the atomic C in the stable hcp(low) site, we find a small attractive interaction, however, if the CH is placed in a hcp(low) site a strong repulsive interaction of 0.72 eV results. Thus C and CH co-adsorption in neighbouring hcp(low) sites is excluded. Based on the above we therefore assign the 283.55 eV C1s peak on Rh(553) to C-atoms situated in the hcp site at the bottom of the steps.

We now turn to the issue of dissociation of CH on the two surfaces and show in Fig. 5 the result of an extensive search for low energy paths for the dissociation of CH on Rh(111) and Rh(553). As seen, clear differences exist between the two surfaces. On Rh(111), CH starts at hcp hollow site, and dissociates via a transition state with barrier of 0.96 eV, where CH becomes parallel to surface and H sits on top of the nearby Rh atom. The results agree well with Ref. [29]. On Rh(553), CH starts out at the fcc(up) site and ends with the C atom at the hcp(low) site and the H on top of the nearby Rh atom with a barrier of 0.59 eV. These energy barriers on their own would be sufficient for explaining why dissociation at room temperature occurs on Rh(553) and not on Rh(111). In addition to this, Fig. 5 also shows that CH dissociation on Rh(111) is endothermic whereas it becomes slightly exothermic on Rh(553). Thus not only kinetics but also energetics favour the observed behaviour of CH dissociation at the steps of the Rh(553) surface and stability of CH on the flat Rh(111) surface. The driving force originates from the significant stabilization of

atomic C at stepped Rh(553), seen in Table 2. We note that a recent calculation [31] for Ni found a similar behaviour with the slightly endothermic dissociation of CH on Ni(111) becoming exothermic on the stepped Ni(211) surface.

4. Summary and conclusions

The adsorption of ethanol at room temperature on the Rh(111) and its vicinal surface Rh(553) has been investigated by a detailed analysis of high resolution core level spectroscopy data including comparison to calculated C1s binding energy shifts. Extensive DFT-based simulations of adsorption structures and transition states were used to address issues related to the different stability of CH fragments on the two surfaces.

Both surfaces were found to predominantly dissociate the carbon–carbon bond and preserve the carbon–oxygen bond leading to adsorbed CO but no adsorbed atomic O. In addition to CO, also significant amounts of methylidyne and ethylidyne are formed on Rh(111), the latter presumably via a reforming reaction. No significant amounts of atomic C is formed on Rh(111) indicating incomplete dehydrogenation. On Rh(553), the dominant surface species in addition to CO was shown to be atomic C adsorbed in the hcp sites on the lower side of the steps. The surprisingly high C1s binding energy of such C-atoms was reproduced by calculations. The finding of significant amounts of atomic carbon on Rh(553) demonstrates that for this surface, dehydrogenation can proceed beyond the formation of methylidyne. In agreement with the experimental results, DFT-based simulations demonstrated that the activation barrier for CH dissociation was lowered from 0.96 eV on Rh(111) to only 0.59 eV at the Rh(553) steps and furthermore that the CH dissociation changes from endothermic on Rh(111) to exothermic on Rh(553). The large differences in kinetic barriers as well as the energetics show that ethanol adsorption and decomposition on small Rh particles with their large concentration of low-coordinated edge and corner atoms are not well described by the flat Rh(111) surface. The under-coordinated atoms at steps are necessary in order to obtain complete dehydrogenation of the ethanol.

Acknowledgements

This work has been financially supported by the Swedish Research Council and by the Knut and Alice Wallenberg Foundation. Support by the MAX-lab staff is gratefully acknowledged. Wei-Xue Li gratefully acknowledge the financial support from the NSFC 20503030, 20733008 and MOST 2007CB815205.

References

- [1] G.A. Deluga, J.R. Salge, L.D. Schmidt, X.E. Verykios, *Science* 303 (2004) 993.
- [2] S. Cavallaro, V. Chiodo, A. Vita, S. Freni, *J. Power Sources* 123 (2003) 10.
- [3] Hyun-Seog Roh, Yong Wang, David L. King, Alexandru Platon, Ya-Huei Chin, *Catal. Lett.* 108 (2006) 15.
- [4] F. Frusteri, S. Freni, L. Spadaro, V. Chiodo, G. Bonura, S. Donato, S. Cavallaro, *Catal. Commun.* 5 (2004) 611.
- [5] M.M. Yang, X.H. Bao, W.X. Li, *J. Phys. Chem. C* 111 (2007) 7403.
- [6] J.N. Andersen, A. Beutler, S.L. Sorensen, R. Nyholm, B. Setlik, D. Heskett, *Chem. Phys. Lett.* 269 (1997) 371.
- [7] M. Wiklund, A. Beutler, R. Nyholm, J.N. Andersen, *Surf. Sci.* 461 (2000) 107.
- [8] T. Fuhrmann, M. Kinne, C.M. Whelan, J.F. Zhu, R. Denecke, H.-P. Steinrück, *Chem. Phys. Lett.* 390 (2004) 208.
- [9] H.-P. Steinrück, T. Fuhrman, C. Papp, B. Tränkenschuh, R. Denecke, *J. Chem. Phys.* 125 (2006) 204706.
- [10] R. Nyholm, J.N. Andersen, U. Johansson, B.N. Jensen, I. Lindau, *Nucl. Instr. Meth. Phys. Res. A* 467–468 (2001) 520.
- [11] A. Resta, J. Blomquist, J. Gustafson, H. Karhu, A. Mikkelsen, E. Lundgren, P. Uvdal, J.N. Andersen, *Surf. Sci.* 600 (2006) 5136.
- [12] J.E. Bartmess, R.M. Georgiadis, *Vacuum* 33 (1983) 149.
- [13] S. Doniach, M. Šunjić, *J. Phys. C* 3 (1970) 285.
- [14] U. Gelius, S. Svensson, H. Siegbahn, E. Basilier, Å. Faxälv, K. Siegbahn, *Chem. Phys. Lett.* 28 (1974) 1.

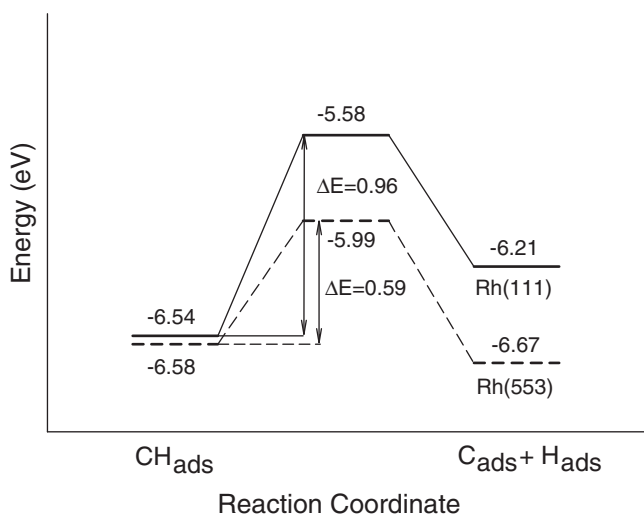


Fig. 5. Potential energy surfaces (referenced to a CH radical in gas phase) for the initial state (left), the transition state (middle), and the final state (right) for the lowest energy dissociation paths on Rh(111) (solid lines) and Rh(553) (dashed lines). The activation energies (ΔE) for the two surfaces are indicated. All energies are in eV.

- [15] S. Cederbaum, W. Domcke, *J. Chem. Phys.* 64 (1976) 603.
- [16] B. Hammer, K.W. Jacobsen, V. Milman, M.C. Payne, *J. Phys.: Condens. Matter* 4 (1992) 453.
- [17] D. Vanderbilt, *Phys. Rev. B* 41 (1990) 7892.
- [18] M. Birgersson, C.-O. Almbladh, M. Borg, J.N. Andersen, *Phys. Rev. B* 67 (2003) 045402.
- [19] L. Köhler, G. Kresse, *Phys. Rev. B* 70 (2004) 165405.
- [20] J.G. Wang, W.X. Li, M. Borg, J. Gustafson, A. Mikkelsen, T.M. Pedersen, E. Lundgren, J. Weissenrieder, J. Klíkovits, M. Schmid, B. Hammer, J.N. Andersen, *Phys. Rev. Lett.* 95 (2005) 256102.
- [21] M.M. Yang, X.H. Bao, W.X. Li, *J. Chem. Phys.* 127 (2007) 024705.
- [22] J.P. Perdew, J. Chevary, S. Vosko, K.A. Jackson, M.R. Pederson, D. Singh, C. Foilhais, *Phys. Rev. B* 46 (1992) 6671.
- [23] M. Smedh, A. Beutler, T. Ramsvik, R. Nyholm, M. Borg, J.N. Andersen, R. Duschek, M. Sock, F.P. Netzer, M.G. Ramsey, *Surf. Sci.* 491 (2001) 99.
- [24] J.N. Andersen, A. Resta, E. Lundgren, J. Gustafson et al., in press.
- [25] R. Larciprete, A. Goldoni, A. Groso, S. Lizzit, G. Paolucci, *Surf. Sci.* 482 (2001) 134.
- [26] C.M. Whelan, R. Neubauer, D. Borgmann, R. Denecke, H.P. Steinrück, *J. Chem. Phys.* 115 (2001) 8133.
- [27] *Handbook of X-ray Photo Emission Spectroscopy*, Perkin Elmer, 1978.
- [28] S.J. Osborne, S. Sundin, A. Ausmees, S. Svensson, S.L. Sorensen, L.J. Saethre, O. Svaeren, J. Végh, J. Karvonen, S. Aksela, A. Kikas, *J. Chem. Phys.* 106 (1997) 1661.
- [29] B.S. Bunnik, G.J. Kramer, *J. Catal.* 242 (2006) 309.
- [30] C. Papp, B. Tränkenschuh, R. Streber, T. Fuhrmann, R. Denecke, H.-P. Steinrück, *J. Phys. Chem. C* 111 (2007) 2177.
- [31] H.S. Bengaard, J.K. Nørskov, J. Sehested, B.S. Clausen, L.P. Nielsen, A.M. Molenbroek, J.R. Rostrup-Nielsen, *J. Catal.* 209 (2002) 365.